Multiwavelength and polarization lidar sounding of industrial aerosol emissions

S.S. Khmelevtsov,[1] V.A. Korshunov,[1] V.M. Nikitin,[2] and V.V. Kobelev[2]

[1] *Scientific-Production Association "Typhoon", Obninsk, Kaluga Region*
[2] *Belgorod State University*

Received December 20, 2004

Cement aerosol plume has been probed by means of a three-wavelength (355, 532, and 1064 nm) and polarization (532 nm) lidar. The depolarization ratio of lidar return from aerosol particles observed outside the visible part of the plume in the area of turbulent pollutant dispersal is near 40%. Characteristic equivalent radius of particles retrieved from lidar measurements of the extinction coefficients is 0.9 μm. Mass concentration as a function of the distance from the aerosol source is presented. Results on the aerosol mass concentration measured with lidar are in a reasonably good agreement with known published data of numerical modeling and *in situ* measurements.

Introduction

Pollution of the atmosphere over big industrial centers by aerosol and gas emissions has unhealthy influence on human beings and environment. The complex of measures to decrease the level of this pollution should include adequate tools for monitoring of the emissions. The remote methods for monitoring are not the last among them, in particular, the lidar methods. In this paper we consider the possibility of applying multiwavelength and polarization lidar sounding to monitoring of the characteristics of aerosol emissions generated at cement production. The study was carried out in the industrial area of the city of Belgorod, where a big cement plant is situated.

As known, calibration of lidar is the essentially necessary part of lidar measurements. When sounding atmospheric aerosol, the lidar is most often calibrated by means of the reference of the signals to the backscattering coefficients at the points of the path, where they are assumed known. The reference points are usually selected in the high layers of the atmosphere, where the backscattering coefficient is close to the Rayleigh one. In sounding urban aerosol, in particular, the plumes of aerosol emissions, the sounding is performed along slant paths at a relatively low elevation angles, and reference to high altitudes is not realistic because of extinction of radiation along the path. It makes some difficulties in calibration of the lidar.

An alternative approach to sounding of aerosol emissions spreading as an aerosol plume is based on determination of the extinction coefficients.[1,2] In Ref. 1 the optical thickness of the plume is determined by comparing the signals before and behind the plume. The assumption is used on homogeneity of the background aerosol atmosphere along the sounding path, and extinction of the signals in the background atmosphere is ignored.

The weaker assumption is used in Ref. 2 that the profile of the background aerosol backscattering coefficient along the sounding path does not depend on the choice of the direction of sounding in some limited range of the sounding angles adjacent to the stack mouth. The optical thickness of the plume is determined by comparing the signals from the background aerosol atmosphere with the signals from the aerosol plume. The method 2 is accepted by American Environmental Protection Agency (EPA) as the official alternative method for determination of the optical thickness of aerosol plume from a stationary smoke source.

Using lidar measurements at a single wavelength, one can monitor the temporal variations of the emission intensity and to determine the spatial field of the emission spread.[3,4] However, according to the actual rules and standards for quantitative estimation of emissions, it is accepted to use the value of the mass (volume) aerosol concentration. The coefficients of relations between the optical and volume aerosol characteristics depend on the microphysical aerosol characteristics and can vary within significant limits.[4]

To take into account the variations of the aerosol microphysical characteristics, it is expedient to use the multiwavelength sounding, which allows determining the extinction coefficients at a few wavelengths. Then the integral aerosol parameters in the plume, in particular, the aerosol mass concentration, can be retrieved by means of solving the inverse problem. As one can expect the presence of nonspherical particles providing noticeable polarization of the backscattering signals in dust emissions,[3–5] makes it meaningful to accompany the multiwavelength sounding with a polarization sounding in order to identify the particle type.

Let us note that the use of the extinction coefficients instead of backscattering coefficients has essential advantages when solving the inverse problem in the case of nonspherical aerosol, because

0235-6880/05/03 212-06 $02.00

the extinction coefficients are less sensitive to the particle shape in comparison with the backscattering coefficients.[6] The possibility of replacing non-spherical particles with spheres of equivalent surface area in calculations of the extinction coefficients depends on the particle size and shape. According to the data from Ref. 6, for the randomly oriented spheroids and cylinders with the parameter $\rho_e = 2\pi r_e/\lambda \geq 5$ (where r_e is the radius of the sphere of the equivalent area and λ is the wavelength) and the moderate shape parameter χ (from 1/2 to 2), the difference appearing due to the replacement is within few percent. So, when solving the inverse problem in the size range meeting the aforementioned condition, one can use the calculations by the Mie formulas for spherical particles. The method for solving the inverse problem should be coordinated with the error of calculations and experimental data. At the errors of the order of a few percent and the number of measured optical parameters no more than four one can expect to retrieve only the integral parameters of distributions, that can be sufficient for solving many applied problems.

Description of the experiment

A multiwavelength MVL-60 mobile lidar mounted in a trailer was used in the experiments. The lidar could operate in two measurement regimes, multiwavelength and polarization. The principal specifications of the lidar are presented below.

In the multiwavelength regime of operation, the receiving block provides operation of four parallel measurement channels. Simultaneous measurements at the wavelengths of 1064, 532, and 355 nm were carried out, and in future it is planned to use the 4th channel for receiving the signals of Raman scattering from atmospheric nitrogen. In the regime of polarization measurements, two components of a lidar return were received at the wavelength of 532 nm with the polarizations, parallel and perpendicular to the polarization of sounding radiation. The transmitting block of the lidar included an LS-2137 laser, the radiation of which was divided into three separate channels with different wavelengths by means of the spectral divider. Each channel was equipped with a beam expander to decrease the divergence of the beam at a magnification factor of 3.6^x. The Glan prism was also installed in the channel of 532 nm, which was used for calibration of the polarization channels. The receiving telescope with the transmitting device was mounted on the alt-azimuth rotated device providing scanning over the elevation angle from −10 to 90° and over azimuth from 0 to 360°.

In sounding, the lidar was placed at a hill at the distance about 2 km to the south from the stacks of the cement enterprise compactly situated on the area of 100 × 100 m. The highest stack height was 100 m. Another source of dust aerosol was situated at the distance of about 900 m to the west from the stacks. At eastward wind direction it generated an additional spread of dust aerosol cloud. Mean temperature of dust–gas components emitted from the stacks to the atmosphere, according to the production technology, was 100°C, and the speed of their emission from the stack mouth was on the order of 5 m/s. Condensation of water vapor occurred resulting from mixing with cold air, and the visible aerosol plume was formed, which expanded as moving from the source. Sounding of the visible part of the plume is feasible because water droplets formed due to condensation make the principal contribution to backscattering.

To estimate the dust aerosol emissions, sounding was carried out in the turbulent scattering zone out of the visible observed plume. The diagram of the experiment is shown in Fig. 1*a*.

Principal specifications of the lidar

Transmitter	
Laser	LS-2137
Wavelengths, nm	1064, 532, 355
Pulse energy, mJ at the wavelength of, nm	
...	1064 550
...	532 300
...	355 120
Pulse repetition rate, Hz	from 1 to 10
Laser radiation pulse duration at the level of 0.5, ns	no more than 15–17
Angular divergence of the laser beam at the level of 0.5, arc min.	no more than 2
Receiver	
Diameter of the main telescope mirror, mm	600
Telescope field of view, arc min.	2 – 10
Number of receiving channels	2 – 4
Transmission band of the interference filters at the level of 0.5, nm	2 – 5
Regime of signal processing	analog
Photoreceivers	PEM-83 (1), PEM-100 (3)
ADC	two 25 MHz / 12 bit, two-channel

The lidar was placed at the point L, the sounding directions LX and LY are different in the azimuth at a constant elevation angle. The path LX is located in the area free of aerosol pollution and provides the background backscattering signal $P_X(R)$ from the "clean" atmosphere depending on the distance R along the sounding path. The sounding path LY is located in the admixture dispersal zone and provides the signal $P_Y(R)$.

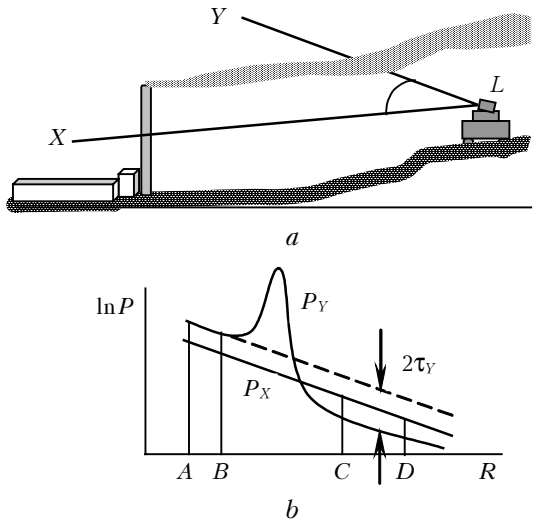

Fig. 1. To the technique for determination of the optical thickness of aerosol plume: diagram of the experiment: sounding under the plume along the path LY gives the signal P_Y; sounding of the "clean atmosphere" along the path LX gives the signal P_X (*a*); determination of the optical thickness of the plume from comparison of the signals PY and PX (*b*).

Technique of the multiwavelength measurements

The technique for determination of the optical thickness of an aerosol plume and its mean extinction coefficient is illustrated by Fig. 1*b*. The path segments AB and CD are the segments for comparison of the signals P_X and P_Y before and behind the plume. It is assumed that the signals are corrected for the square of the distance. Then the relationship between the signals P_X and P_Y for the segments AB and CD can be represented in the following form:

$$(AB)\ \ln P_Y(R) + K + \delta(\ln P_Y(R)) = \ln P_X(R),$$
$$(CD)\ \ln P_Y(R) + K + \delta(\ln P_Y(R)) = -2\tau_Y + \ln P_X(R), \qquad (1)$$

where τ_Y is the optical thickness of the plume, K is the constant independent of R responsible for the changes occurring between sounding along the paths LX and LY including, for example, the change of energy of the transmitted pulses by the lidar transmitter, large-scale variations of the state of the aerosol medium, the change of the atmospheric transparency along the path segment from the lidar to the point A, etc., $\delta(\ln P_Y(R))$ are the signal fluctuations caused by the error in recording the signals and the small-scale (in comparison with the distance between the points A and D, as well as the distance between the paths LX and LY) fluctuations of the optical characteristics of the background aerosol medium.

Ignoring the fluctuations, the following relationship for determining τ_Y follows from expression (1):

$$\tau_Y = 0.5[\langle \ln P_Y(R) - \ln P_X(R)\rangle_{AB} - \langle \ln P_Y(R) - \ln P_X(R)\rangle_{CD}], \qquad (2)$$

where $\langle\ \rangle$ means averaging over the segments AB or CD. Fluctuations of the signal $\delta(\ln P_Y(R))$ are the sources of the errors in measurements of $\delta\tau_Y$. Calculation of fluctuations depending on the atmospheric conditions is quite a difficult task. One can estimate the error $\delta\tau_Y$ based on the model experiment including a few successive soundings along the path LX. When processing the data obtained, one of the soundings is assumed to be the background, and the optical thickness of the other is determined by formula (1), and then they give the estimate of the error $\delta\tau_Y$. In particular, according to the results of such experiment in anticyclonic conditions $\delta\tau_Y = 0.02$.

Together with $\tau_Y(\lambda)$, the mean extinction coefficients at the wavelengths of sounding were determined in the aerosol plume $\sigma(\lambda) = \tau_Y(\lambda)/\Delta R$, where ΔR is the characteristic size of the aerosol plume at the half maximum level. The set of $\sigma(\lambda)$ at three wavelengths 355, 532, and 1064 nm was used for determination of the integral aerosol parameters.

Let us consider the possibilities of determining the characteristic particle size from measurements of the extinction coefficients at the aforementioned wavelengths. Two parameters can be obtained from the extinction coefficients, which depend only on the size, but not on the number density of particles. They are the ratios

$$R_{12} = \sigma(355)/\sigma(532) \text{ and } R_{13} = \sigma(355)/\sigma(1064).$$

The curve $\{R_{12}(r_0),\ R_{13}(r_0)\}$, where r_0 is the median radius of the lognormal distribution

$$f(r) = r^{-1}\exp[-(\ln r/r_0)^2/(2\rho^2)]$$

(r is the particle radius) with the parameter $\rho = 0.2$, which corresponds to a narrow size distribution, is shown in Fig. 2 on the plane (R_{12}, R_{13}) in a parametric form.

Calculations were made for the refractive index $n = 1.55 - 0.005i$. The general shape of the dependences is the same for other refractive indices in the range n from 1.35 to 1.6. The parameter r_0 varied in the range 0.05–3 μm, the values r_0 for some points are shown in Fig. 2.

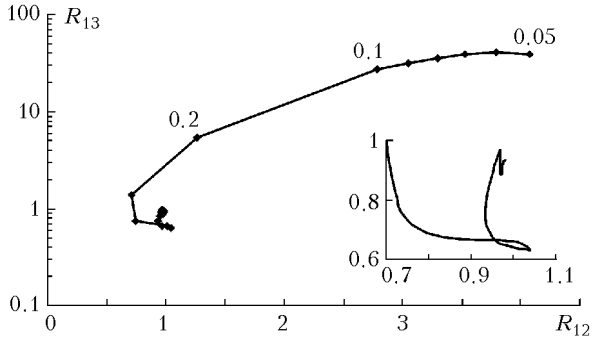

Fig. 2. Parametric dependence of the ratios of the extinction coefficients $\{R_{12}(r_0), R_{13}(r_0)\}$ on r_0 (the median radius of the lognormal particle size distribution). The radius r_0 varies in the limits 0.05 (0.01) 0.1 and 0.1 (0.1) 1.5 μm. The fragment of the general dependence on a larger scale is shown in the lower right corner of the figure.

It follows from Fig. 2 that the variations of R_{13} and R_{12} separately cannot provide for an unambiguous determination of the particle size in the range 0.05–3 μm. At simultaneous measurement of R_{13} and R_{12} unambiguous determination of the size is possible in the case when the curve $\{R_{12}(r_0), R_{13}(r_0)\}$ is not self-crossing. In this case, as is seen in Fig. 2, the curve has not self-crossing points from 0.05 to 3 μm except for a small loop in the region of 0.5–0.7 μm. As the loop area is small, here one cannot say about the ambiguity, but rather about an increase in the errors of determination of the particle size in the range 0.5–0.7 μm.

Analysis of data shown in Fig. 2 shows that the loss of measurement sensitivity to the particle size from the side of large particles occurs in the range 1.5–2 μm. Thus, there is the principle possibility of estimating the particle size, at least, in the class of single-mode distributions in the characteristic size range from 0.05 to 1.5–2 μm.

To obtain preliminary data on the characteristic particle size, the particles were sampled, detained in the last of aerosol filters of electrostatic type installed in the stack of the enterprise. The sampled particles were sprayed to the plate and analyzed with a microscope. It occurred that the majority of particles have the size in the range from 2 to 4 μm and the elongated shape, and the degree of elongation (the ratio of the maximum size to minimum) does not exceed 3. Then one can conclude that the aerosol particles emitted from the stack have the size, at least, not exceeding 4 μm (or the radius not greater than 2 μm at replacing them by equivalent spheres). Thus, according to the preliminary data, the particle size should not lie out of the range of sensitivity of lidar measurements.

According to the measured results on the optical thickness at three wavelengths, the particle size distribution function was retrieved and then the integral parameters were calculated. The combined method was used for retrieval of the size spectrum. It included 1) parameterization of the spectrum with subsequent selection of the optimal parameters; and 2) the method for regularization with selection of the regularization parameter by the discrepancy.

The lognormal distribution was used at the parameterization stage. The solution was corrected by the regularization method at unsatisfactory (from the standpoint of the discrepancy) result of optimization. The volume concentration V ($\mu m^3/cm^3$) and the characteristic radius r_{32} (μm) (the ratio of the third moment of the distribution to the second) were calculated from the determined distribution. Let us note, that the radii of nonspherical particles equivalent in the surface area and in the volume do not coincide, but this difference for moderately elongated (oblate) spheroids and cylinders ($1/2 \le \chi \le 2$) does not exceed 5% (Ref. 6) that makes it possible to calculate V ignoring the particle shape.

This algorithm for retrieving the integral parameters was tested in the numerical experiment. Different functions, including the logarithmic normal distribution, as well as the single-mode convex function of more general type were taken as the initial size distributions. When considering the initial distributions, the characteristic radius r_{32} varied from 0.5 to 2 μm. The obtained errors in retrieving the volume concentration were 15–20% in the absence of the errors in the experimental data and increased to 30–40% at introducing a 20% error into the measurement data on the extinction coefficients.

Measurement results and their discussion

a) Polarization measurements

Examples of the results obtained from polarization sounding data are shown in Fig. 3 for three characteristic cases of sounding, including sounding of a clean atmosphere (Fig. 3*a*), visually observed aerosol plume emitted from the stack (Fig. 3*b*), and the aerosol cloud near the plume (Fig. 3*c*).

The backscattering signal $P_\parallel$ with polarization parallel to the initial one is shown in Fig. 3 in relative units, as well as the degree of depolarization of the backscattering signal $d = P_\perp / P_\parallel$. The degree of depolarization of the signal in the clean atmosphere (Fig. 3*a*) is approximately constant along the sounding path and varies about 0.07. The peak of d is observed in the plume (Fig. 3*b*) and under the plume (Fig. 3*c*). It is seen in Fig. 3*b* that the value d_2 is constant in the front part of the visible plume up to the maximum, and then it begins to quickly increase. Such a behavior of d is characteristic of liquid-droplet media, and the increase of d is related to the effect of multiple scattering in the plume.

The calculated result on the degree of depolarization for the clean atmosphere and for the aerosol admixture is shown in Fig. 3*c*. In this case, the signal from clean atmosphere was extrapolated to the region of admixture, and the ratio $G = P_{\parallel 1} / P_{\parallel 2}$

was calculated, where the index 1 is related to the extrapolated signal, and the index 2 is for the aerosol admixture. Based on the fact that the measured value $d = (P_{\perp 1} + P_{\perp 2})/(P_{\parallel 1} + P_{\parallel 2})$, it is easy to obtain that $d_2 = d + G(d - d_1)$, where d_1 is the degree of polarization for the clean atmosphere extrapolated to the region of admixture, d_2 is the degree of depolarization for the admixture. The quantity $d_2(R)$ calculated in this way is also shown in Fig. 3*c*.

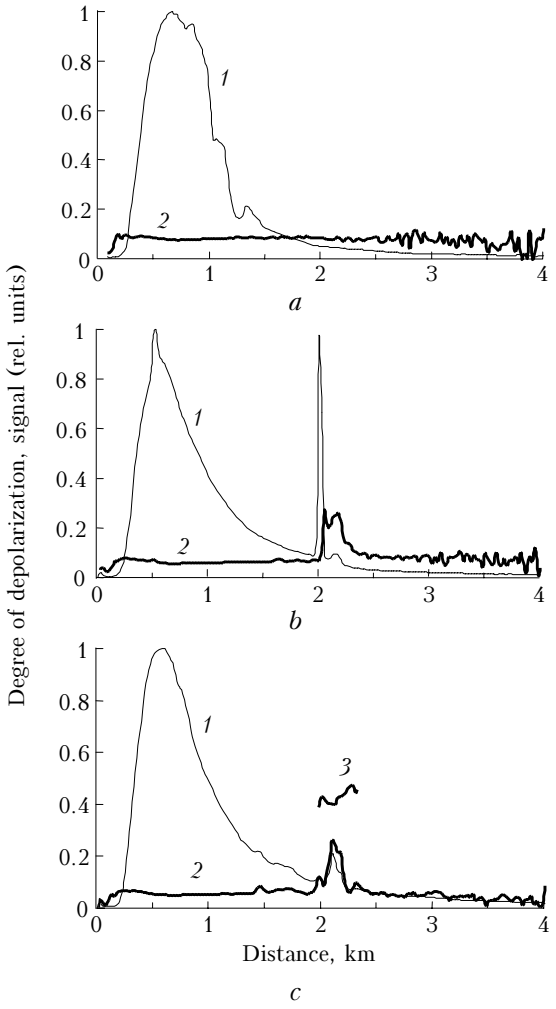

Fig. 3. Backscattering signals with polarization parallel to the initial one, $P_{\parallel}$, rel. units (*1*), and the profiles of the degree of depolarization d (*2*) for the case of sounding of the "clean" atmosphere (*a*), visually observed part of the plume (*b*) and the zone of turbulent spread of admixture out of the visible part of the plume (*c*). Curve *3* (*c*) shows calculation of the degree of depolarization of the backscattering signal from only admixture d_2.

The degree of depolarization $d_2(R)$ in the region of the aerosol cloud under the plume (Fig. 3*c*) is ≈ 0.4 and weakly changes across the plume. These results are typical for all measurements of the aerosol degree of depolarization out of the visible plume: the value d_2 varies in narrow limits from 0.39 to 0.42. Let us note that close values of the degree of depolarization 0.4–0.45 were obtained in the region out of the visible part of the plume of the electric power plant smoke cleaned with filters.[3] The high values of the depolarization coefficient obtained show that the degree of humidification of cement dust particles out of the plume is insignificant. Let us note that in the majority of events relative humidity of air during sounding did not exceed 55%.

It is interesting to compare the results of field lidar measurements with the data[5] on the degree of depolarization for indoor dust aerosol and cement dust. For cement dust $d = 0.56$ just after spraying, then 5 minutes later, after sedimentation of the largest particles, the value d stabilizes at the level of 0.40–0.42, which is in a good agreement with the aforementioned data. The measured d values also do not contradict the calculated data.[6] Indeed, according to the results of three-wavelength measurements (see below), the value of the parameter $\rho_e = 10$ is characteristic of the sounded cement dust. According to data from Ref. 6 the maximum d values are reached in the range $\rho_e = 5$–10, and the calculated d values at $\rho_e = 10$ and at some values of the shape parameter (for example, 2 or 1/2 for cylinders and 1.4 for spheroids) approaches to the measured value $d = 0.4$.

b) Three-wavelength sounding

Preliminary data processing has shown that significant fluctuations of the parameters of aerosol plume take place depending on orientation of the sounding path with respect to the plume axis. The optical thickness varies in the limits 0.05–0.6, geometric size at the level of 0.5 of the maximum changes from 50 to 700 m, and the mean extinction coefficient at $\lambda = 532$ nm – from 0.1 to 4 km^{-1}. The ratios of the extinction coefficients $\sigma(355)/\sigma(532)$ vary in the range from 0.7 to 1.2, $\sigma(355)/\sigma(1064)$ – from 0.5 to 1.1. It is obtained from the retrievals of the integral parameters that the characteristic radius $r_{32} = (0.9 \pm 0.3)$ μm, and the relation coefficients between the extinction coefficient and the mass concentration are (1.3 ± 0.4), (1.3 ± 0.6), and (1.2 ± 0.4) mg·km/m^3 for the wavelengths of 355, 532, and 1064 nm, respectively. Let us note that, according to data from Ref. 4, the relation coefficients vary in the limits 0.1–1.5 mg·km/m^3 depending on the aerosol type. It is explained by the fact that the cement dust particles are relatively larger than the particles of industrial pollution generated in condensation processes.

The measured mass concentration in the aerosol plume is shown in Fig. 4 as a function of the distance along the direction of aerosol transport. The measurement data obtained at the level of 70–100 m over the ground surface were used.

The solid curve shows the mean (over the distance range of 250 m) dependence. The distance is read from the stack group center along the wind direction, negative distances are related to the data from the windward side. The mean value of the mass

concentration in the distance range 1–1.5 km is 620 μg/m^3.

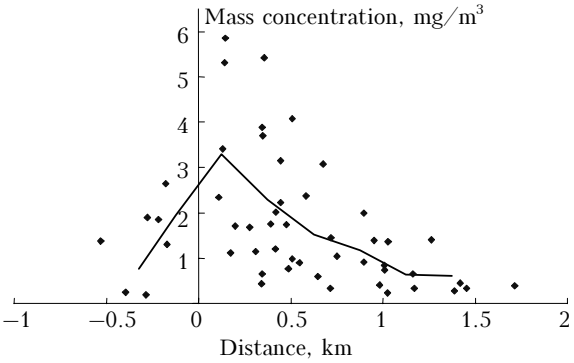

Fig. 4. Lidar measurement data on the mass concentration of cement dust at the level of 70–100 m over the ground surface as a function of the distance from the stack group (rhombs show individual measurements, and the line shows the mean dependence over the interval of 250 m).

Let us compare the obtained results with the calculated and measured data.[7] According to the experimental data[7] the near-ground concentration of admixture emitted from cement enterprise at the distance of 1–2 km is $2 \cdot 10^{-6}$ [s/m^3]M, where M [g/s] is the outcome of the emission per time unit. At the same time, according to the results of numerical simulations, the ratio of concentrations of the admixture at the level of 80 m to the near-ground concentration at the same distances is equal to 3. Combining these data and taking the estimate M = 90 g/s received from the data of the enterprise, we obtain the value of the mass concentration of 540 μg/m^3, which is in a satisfactory agreement with the results of lidar measurements.

Conclusions

Polarization and three-wavelength lidar sounding of aerosol emission of a cement enterprise has been carried out. It is obtained from the results of sounding, that the visually observed part of the plume is a dense aerosol formation with the prevalence of spherical water droplets. The presence of admixture is observed out of the visible part of the plume, spread due to the turbulent diffusion. Depolarization of the signal from admixture is 40% that corresponds to the data of earlier model experiments on the backscattering from cement dust. According to data of three-wavelength sounding, the characteristic value of the equivalent particle radius is (0.9 ± 0.3) μm.

The mass concentration of the admixture has been estimated. Comparison with the published results of measurements of the mass concentration of admixture for a cement enterprise and with the data of numerical simulation shows that the lidar data and data of independent measurements on the mass concentration are in a satisfactory agreement. It follows from the results of the work, that the technique investigated in the paper can be applied to monitoring of emissions and determination of the area of spread of the aerosol admixture from cement enterprise and other sources of finely dispersed dust.

Acknowledgments

The work was supported in part by the Ministry of Education of Russian Federation under the project "Creation of inter-institute of high education system of education-scientific centers of collective use for ecological monitoring for stable development of the regions" (2002–2004) and the program of purposeful financial support for development of the instrumentation basis of the scientific research CCU at Belgorod State University (2004).

References

1. C.S. Cook, G.W. Bethke, and W.D. Conner, Appl. Opt. **11**, No. 8, 1742–1748 (1972).
2. *EPA Electronic Code of Federal Regulations*. 40-CFR. P. 60. Appendix A.
3. I.E. Penner and V.S. Shamanaev, Atmos. Oceanic Opt. **7**, No. 3, 178–181 (1994).
4. V.E. Zuev, B.V. Kaul, I.V. Samokhvalov, K.I. Kirkov, and V.I. Tsanev, *Laser Sounding of Industrial Aerosol* (Nauka, Novosibirsk, 1986), 186 pp.
5. A.S. Drofa, V.A. Korshunov, and N.P. Romanov, Trudy Ins. Exp. Meteorol., Issue 26 (161), 24–30 (1996).
6. M.I. Mishchenko, L.D. Travis, and A.A. Lacis, *Scattering, Absorption, and Emission of Light by Small Particles* (Goddard Institute for Space Studies, New York, 2004).
7. M.E. Berlyand, *Modern Problems of Atmospheric Diffusion and Pollution of the Atmosphere* (Gidrometeoizdat, Leningrad, 1975), 448 pp.